Published in final edited form as:
Biomaterials. 2012 March ; 33(8): 2482–2491. doi:10.1016/j.biomaterials.2011.12.004.

Mechanical Derivation of Functional Myotubes from Adipose-Derived Stem Cells

Yu Suk Choi[1], **Ludovic G. Vincent**[1], **Andrew R. Lee**[1], **Marek K. Dobke**[2], and **Adam J. Engler**[*, 1]

[1]Department of Bioengineering, University of California, San Diego, California, USA

[2]Department of Plastic Surgery, University of California, San Diego, California, USA

Abstract

Though reduced serum or myoblast co-culture alone can differentiate adipose-derived stem cells (ASCs) into mesenchymal lineages, efficiency is usually not sufficient to restore function *in vivo*. Often when injected into fibrotic muscle, their differentiation may be misdirected by the now stiffened tissue. Here ASCs are shown to not just simply reflect the qualitative stiffness sensitivity of bone-marrow-derived stem cells (BMSCs) but to exceed BMSC myogenic capacity, expressing the appropriate temporal sequence of muscle transcriptional regulators on muscle-mimicking extracellular matrix in a tension and focal adhesion-dependent manner. ASCs formed multi-nucleated myotubes with a continuous cytoskeleton that was not due to misdirected cell division; microtubule depolymerization severed myotubes, but after washout, ASCs re-fused at a rate similar to pretreated values. BMSCs never underwent stiffness-mediated fusion. ASC-derived myotubes, when replated onto non-permissive stiff matrix, maintain their fused state. Together these data imply enhanced mechanosensitivity for ASCs, making them a better therapeutic cell source for fibrotic muscle.

Keywords

Myogenic differentiation; Skeletal muscle; Mechanotransduction; Extracellular matrix; Stiffness

1. Introduction

Regenerative musculoskeletal applications have been plagued with setbacks owing in part to the fibrosis present in degenerative muscle disorders, e.g. muscular dystrophy [1] which affects 1 in every 3,600 male births [2]. Fibrotic muscle has increased collagen density and transglutaminase activity that stiffens the extracellular matrix (ECM) [1, 3], making it more closely resemble the osteoid environment of bone [4]. Injection of undifferentiated stem cells into diseased muscle, i.e. cellular myoplasty, was thought to ameliorate the disease by restoring dystrophin expression and thus muscle contraction. Instead, aberrant stem cell differentiation in this fibrotic muscle causes calcified lesions to form [5] due at least in part

[*]Correspondence: aengler@ucsd.edu, Phone: 858-246-0678, Fax: 858-534-5722.

Disclosure
The authors indicate no potential conflicts of interest.

to the osteogenic properties of abnormally stiff muscle [6]. Tissue engineered musculoskeletal systems will require significant efforts to understand the stem cell-microenvironment interaction and overcome the fibrosis problem for successful stem cell engraftment in damaged muscle.

Adult human bone marrow-derived stem cells (BMSCs) [7] are a commonly used cell source for cellular myoplasty since these cells differentiate into myocytes when exposed to myogenic growth factors and express functional dystrophin. They can also be transplanted and detected over an extended time period [8]. However, these cells have not been shown to be myogenic in fibrotic muscle *in vivo* [5, 9, 10] or even to form fused skeletal muscle *in vitro* [4]. While skeletal muscle precursors can engraft into dystrophic muscle [11], limited availability despite expansion capability on compliant matrices [12] may adversely impact their clinical translation. Adult human adipose-derived stem cells (ASCs) are readily available, easily isolated, can be chemically differentiated into myocytes, and are competent to engraft in fibrotic muscle whereas BMSCs are not [10, 13, 14]. While ASCs may appear better suited for translation, functional muscle recovery with these cells is still limited [10], possibly by the stiff diseased environment [1, 6, 15].

In recent years, ECM stiffness has been identified as another potent stem cell differentiation regulator; cell fate is regulated by contraction against their soft or stiff niche [12, 16]. Successful stem cell-based therapies will require acclimating cells to the abnormally stiff ECM of muscular dystrophy [1, 3] while inducing and/or maintaining myogenesis, fusion, and dystrophin delivery. Here we directly compare ASC to BMSC stiffness responsiveness and show that on matrices that mimic skeletal muscle. These data suggest ASC could serve as a viable cell source for fibrotic muscle therapies.

2. Materials and Methods

2.1. Cell Isolation and Culture

Human ASCs were isolated from freshly aspirated human subcutaneous adipose tissue (donor age between 26 and 31 years) according to the method described previously [17–19] with approval of UCSD human research protections program (Project #101878). Liposuction samples (300 ml) were washed extensively with equal volumes of phosphate-buffered saline (PBS), and then incubated at 37°C for 45–60 min in 0.1% type I collagenase (Worthington Biochemical). Enzyme activity was neutralized with Dulbecco's modified Eagle's medium (DMEM)-low glucose (Invitrogen), containing 10% fetal bovine serum (FBS; Thermo Scientific) and 1% antibiotic/antimyocotic (Invitrogen). Cells were centrifuged at 1200 rpm for 10 min to remove adipocytes. The pellet was resuspended in 0.16 M NH_4Cl and incubated at room temperature for 5 min to lyse red blood cells. Cells were collected by centrifugation at 1200 rpm for 5 min, filtered through a 100 μm nylon mesh to remove fissile debris, and incubated overnight on tissue culture plastic in complete medium at 37°C and 5% CO_2. Plates were then washed extensively with PBS to remove residual non-adherent cells. To reduce donor to donor variation, cells from three different donors were pooled. BMSCs (Lonza Walkersville) were cultured in low glucose DMEM with either 10 or 20% FBS and 1% antibiotic/antimyocotic as indicated. C2C12 skeletal myoblasts (ATCC) were cultured in high glucose DMEM 10% FBS and 1% antibiotic/antimyocotic unless cell fusion was induced in which case serum concentration was reduced to 2%. Stem cells were used at low passage numbers between 4 to 7 and C2C12 cells were sub-cultured below passage number 10. Myoseverin (Calbiochem) was dissolved in dimethylsulfoxide (DMSO) and used at 20 μM for a period of 18 hours before washout. ASCs were fed by new complete medium for another 7 days before fixation [20]. DMSO only was used as negative control.

2.2. Fabrication of Compliant Substrates with Varying Stiffness

Acrylamide was polymerized on an aminosilanized, 25 mm diameter coverslips according to previously established protocol. Briefly, a solution containing the crosslinker N,N' methylene-bis-acrylamide, acrylamide, 1/200 volume of 10% Ammunium Persulfate and 1/2000 volume of N,N,N',N'-Tetramethylethylenediamine was mixed. Three different combinations of acrylamide and bis-acrylamide made 1, 10 and 34 kiloPascal (kPa; unit of stiffness) substrates based on a previous recipe [21]. Approximately 20 μl of the mixed solution was placed on the aminosilanized coverslip and a second coverslip pre-treated with dichlorodimethylsilane was added to ensure to ensure easy detachment and a uniform matrix surface once polymerized. Final matrices were 50 μm thick as measured by microscopy. 10 μg/ml fibronectin was chemically crosslinked using a photoactivating crosslinker, Sulfo-SANPAH (Pierce) and attachment was confirmed by fluorescence. Matrix stiffness was confirmed by atomic force microscopy (AFM; Asylum Research). Cells were seeded onto fibronectin coated samples in 6-well plates at 5×10^2 to 2×10^4 cells per well as needed and cultured for the indicated duration.

2.3. Cell Surface Marker Characterization by Flow Cytometry

ASC and BMSC cultures were trypsinized and resuspended in flow cytometry buffer (PBS supplemented with 2.5% FBS). Cells were incubated with fluorescent-conjugated antibodies against CD34 (Alexafluor 488), CD45 (Alexafluor 488), CD90 (FITC), CD105 (Alexafluor 488) for 30 minutes on ice. Unlabeled cells were incubated with the appropriate isotype control. Cells were analysed using a FACScan (BD Biosciences) using a previous protocol [18].

2.4. Differentiation Assays

Samples were fixed in 3.7% formaldehyde at the indicated time point and selectively stained and imaged as indicated. Morphological changes in three groups (ASC, BMSC 10% FBS, BMSC 20% FBS) were examined by bright field images, and assessment of the development of branches (number of branch per cell) or spindle shapes (the major/minor axis of cell) were quantified using ImageJ software. To quantify matrix mineralization, cells were stained with alizarin red S, and staining was measured spectrophotometrically at 405 nm. Cells also were stained with lineage-specific marker antibodies: neurogenic differentiation with βIII tubulin (Sigma), myogenic differentiaion with Myogenesis Differentiation Protein 1 (MyoD; Santa Cruz Biotech.), and osteogenic differentiation with Runt-related transcription factor 2/Core Binding Factor α1 (Runx2; Alpha Diagnostic International). To measure mRNA transcription level, two specific primers were used per lineage: Microtubule-associated protein tau (MAPT) and Glial cell-derived neurotrophic factor (GDNF) for neurogenesis, myogenic factor 4 (Myogenin) and Myocyte-specific enhancer factor 2C (MEF2C) for myogenesis; Twist transcription factor 1 (TWIST) and bone gamma-carboxyglutamic acid-containing protein (Osteocalcin) for osteogenesis.

2.5. Fusion Assays

ASCs, BMSCs, and C2C12 cells were each divided into two populations, labeled either green (PKH67) or red (PKH26) hydrophobic dyes that localize to the plasma membrane, and seeded onto 10kPa PA matrices for one week. The continuous cytoskeletal structure of fused cells was confirmed by staining for β tubulin (Development Studies Hybridoma Bank) and proliferation marker Ki67 (Santa Cruz Biotech.) was used to identify proliferating binucleated cells. Fusion frequency was determined for the indicated conditions. Myoseverin (Santa Cruz Biotech.) was used to depolymerize microtubules to cause cell fission. To quantify myotube formation, we observed more than 660 cells from four

independent samples. Only binucleated cells with continuous cytoskeleton but lack of Ki67 staining were considered as myotubes.

2.6. Mechanosensing Assays

Vinculin antibody (Sigma) and rhodamine-phalloidin (Invitrogen) was used to visualize focal adhesions and actin, respectively. Strain energy and tangential stress were calculated by TFM as previously described [22]. To knockdown integrin-fibronectin interaction, ASCs were treated by lipid-mediated siRNA (integrin α5 or αV) for 4 days and replated onto 10 kPa matrices for another week. Integrin knockdown effect was determined by flow cytometry using a FACScan (Becton Dickenson).

2.7. Morphological Measurements

Quantitative cell measurements were made using brightfield images from a Nikon Eclipse TE2000-U microscope with a motorized, programmable stage using a CoolSnap HQ camera controlled by Metamorph 7.6 software. Image J software (NIH) was used to analyze images and quantify cell morphology. Specifically, the number of branch points per cells was counted if the branch was longer than the length of the cell's major axis by modified method form previous protocol [23]. The spindle factor was calculated for cells on the indicated matrices as the length of the cell's major divided by its minor axis [4].

2.8. Alizarin Red S and Immunofluorescent staining

Cells were fixed with 3.7% formaldehyde (Sigma) at room temperature for 15 minutes. Samples to be stained by alizarin red were then washed once with dH_2O and 2 ml ARS solution (2%, pH 4.2) was added to each well. ARS solution was removed 1 hour later and each well was washed with dH_2O for 4 to 5 times. Images were taken at this point and the plate was then air dried at room temperature. The amount of matrix mineralization was determined by dissolving the cell-bound ARS in 10% acetic acid and quantifying it spectrophotometrically at 405nm. Samples to be stained immunofluorescently were treated with PBS containing 1% Triton X-100 for 15 minutes and washed with a staining solution of PBS containing 1 μM $MgCl_2$. The primary antibodies listed below with their indicated dilutions in a staining solution containing 2% bovine serum albumin were then added to samples: βIII tubulin (1:100; Sigma), MyoD (1:100; Santa Cruz), Runx2 (1:100; Alpha Diagnostic International), β tubulin (1:100; Developmental Studies Hybridoma Bank), vinculin (1:100; Abcam), and Ki67 (1:100; Santa Cruz Biotechnology). Antibodies were incubated with samples for 30 minutes at 37°C. After washing three times with the staining solution, samples were incubated with Alexa fluor 488- or 568-conjugated secondary antibody (1:400; Invitrogen) for 30 minutes at 37°C. After washing three times with staining solution, nuclei were stained by Hoechst 33342 (1:1000; Invitrogen) for 2 minutes. All samples were examined by a CARV II confocal microscope (BD Biosciences) mounted on a Nikon Eclipse TE2000-U microscope with a motorized, programmable stage using a CoolSnap HQ camera controlled by Metamorph 7.6 software.

2.9. Quantitative Polymerization Chain Reaction (qPCR)

RNA from cells was extracted using a previously published Trizol, chloroform, and isopropanol-based protocol [24]. cDNA was synthesized from the isolated RNA template using Superscript II Reverse transcriptase (Invitrogen), 2.5 mM of random hexamer mix (Invitrogen), and 1 μg of total RNA. The reverse transcription reaction was performed with the following conditions: 37°C for 60 min, 99°C for 5 min, and 5°C for 5 min. The SYBR Green PCR Master Mix (Applied Biosystems) was used with 800 nM of each primer. Primers were custom designed from IDT: MAPT (NM_005910.5) F: 5' ATT ACT GCC AAC AGT TTC GGC TGC 3', R: 5' TAA GAA GGC CCA TGG TGC TGA AGA 3';

GDNF (NM_000514.3) F: 5’ TCC CAT TCA GAG AAC CTT GGC AGT 3’, R: 5’ ACC TGC TTG TGG TGT GTA GGT GAT 3’; Myogenin (NM_002479.4) F: 5’ GCC TTG ATG TGC AGC AAC AGC TTA 3’, R: 5’ AAC TGC TGG GTG CCA TTT AAA CCC 3’; MEF2C (NM_002397) F: 5’ AGT GGG TGG GAA AGG GTC ATT ACA 3’, R: 5’ TAG CCA AGG CTT CTG CTG GTA CTT 3’; TWIST (NM_000474.3) F: 5’ ACC ATC CTC ACA CCT CTG CAT TCT 3’, R: 5’TTC CTT TCA GTG GCT GAT TGG CAC 3’; Osteocalcin (NM_199173.7) F: 5’ TCC AGG CAC CCT TCT TTC CTC TT 3’, R: 5’ GAG TTT ATT TGG GAG CAG CTG GGA 3’. The real-time reaction was done in duplicate in an ABI Prism 7900 HT detection system (Applied Biosystems) using the following reaction profile: 2 min at 50°C and 10 min at 95°C for one cycle, followed by 15 s at 95°C and 1 min at 60°C for 40 cycles. Values were analyzed using SDS 2.3 software (Applied Biosystems), which calculated expression based on a standard curve generated by a fibronectin plasmid [24]. GAPDH was used to normalize all data, which was plotted as a fold change from undifferentiated ASC or BMSC control samples [24].

2.10. Traction Force Microscopy

Strain energy and tangential stresses were calculated by traction force microscopy (TFM) as previously described [22]. Briefly, 30μL of carboxylate-modified 0.1 μm diameter yellow-green fluorescent microspheres (Invitrogen) was added to 1 mL of solution that would create a 10 kPa matrix. Matrices were fabricated, fibronectin functionalized, seeded with 500–2000 cells/well, and cultured for 3 to 7 days. Live cells and embedded tracker particles were imaged by a CARV II confocal microscope (BD Biosciences) mounted on a Nikon Eclipse TE2000-U microscope equipped with a LiveCell chamber (Pathology Devices) and a motorized, programmable stage using a CoolSnap HQ camera controlled by Metamorph 7.6 software. After an image with the cells present was taken, cells were removed by trypsinization, and a second reference image was taken without cells to determine initial bead positions. Using the difference between the two images, matrix deformation was determined from the displacement of the beads. Traction forces were calculated from these deformations and the substrate modulus using a MATLAB script available at http://maeresearch.ucsd.edu/~jalamo/DynaCyte.html. Cell outlines were obtained from phase contrast microscopy using standard image processing techniques.

2.11. RNAi

ASCs were plated onto tissue culture plates in 2% FBS-containing medium and treated with 30nM siRNA with 3ul of siPORT NeoFX (Invitrogen) at the same time. Cells were incubated with either α5 (s7549; Invitrogen) or αV integrin siRNA (s7570; Invitrogen) for 4 days and then replated onto 10 kPa matrices in 10% FBS-containing medium for another 1 to 7 days. Knock-down effects were detected by flow cytometry using FITC conjugated α5 or αV integrin antibodies (BioLegend). ASCs treated only by siRORT NeoFX served as internal negative control.

2.12. Statistical Analysis

All data are expressed as mean ± standard deviation of experiments at least in triplicate with the number of cells analyzed as indicated when possible other than Figure 4C, which shows the mean ± standard error of the mean. Statistical analysis was performed using student t-test, one- or two-way ANOVA on Graphpad Prism software. P-values < 0.05 were considered to indicate statistical significance though p-values < 0.1 are indicated as well.

3. Results

3.1. Matrix elasticity-dependent stem cell fate

Donor-dependent heterogeneity was minimized by pooling cells from multiple donors and sub-culturing. To ensure similar undifferentiated cell states, pooled populations of ASCs and BMSCs were characterized by cell surface marker expression for the presence of mesenchymal markers CD90 and CD105 and the absence of haemopoietic markers CD34 and CD45 [7]. Marker expression in both populations indicated identical mesenchymal cell states (Fig. S1), so we sought to assess whether ASC's differentiation capacity towards neuro-, myo-, and osteogenic lineages was similar to that previously reported for BMSCs [4, 25]. Both populations were initially cultured on fibronectin-coated matrices of 1, 10, and 34 kiloPascal (kPa; Pascal is a unit of stiffness) which mimic the mechanical niche of 'soft' brain, 'firm' muscle, and 'stiff' collagenous bone, respectively [26], and are considered permissive matrices for that lineage. After one week of culture, both qualitative and quantitative ASC morphology mimicked BMSCs; both cell sources appeared well branched on 1 kPa matrices (Fig. 1A, Left images), having developed 50% more branches per cell than on stiffer ones which did not change over time (Fig. 1C). Similar lineage-specific observations were made on firm 10 kPa and stiff 34 kPa matrices for both ASCs and BMSCs in that they resembled elongated myocytes and well-spread osteocytes, respectively (Fig. 1A, Center and right images); spindle shape comparison (Fig. 1D) and alizarin red S, a mineralization indicator (Fig. 1E), were higher on permissive and lower on non-permissive matrices for each lineage. Cells were also fluorescently labeled to detect lineage-specific markers including neurogenic βIII tubulin, the muscle transcription factor MyoD, and the osteogenic transcription factor Runx2 [4]. Both cell sources confirmed expression at inductive matrix stiffness, i.e. neurogenic, myogenic, and osteogenic differentiation on 1, 10, and 34 kPa, respectively (Fig. 1B). βIII tubulin and MyoD showed time-dependent expression and nuclear localization changes, respectively (Fig. S2A and S2B), whereas nuclear-localized Runx2 expression was observed in both cell populations after 1 day in culture (Fig. S2C). Staining on non-permissive matrices for each lineage again was absent (Fig. S3A) consistent with previous lineage commitment [4]. To ensure that stiffness-induced lineage commitment was independent of chemical stimulation, assessment was also performed at multiple serum concentrations; BMSCs did not show serum dependence on expression of any lineage (Fig. 1, 10 vs. 20% serum).

While qualitative differences were not observed, quantitative polymerization chain reaction (qPCR) indicated large gene expression differences over a 2 week time course (Fig. 2). Two markers per lineage were analyzed with results consistent with protein expression (Fig. 1B). On soft matrix, both stem cell sources expressed higher levels of mRNA for microtubule-associated protein tau (MAPT) and glial cell-derived neurotrophic factor (GDNF) relative to undifferentiated controls over time. ASCs showed greater upregulation of MAPT (Fig. 2, Left top) while GDNF had statistically higher expression in BMSCs (Fig. 2, Left bottom). Cells on firm matrices had upregulated Myogenin and myocyte-specific enhancer factor 2C (MEF2C). Though BMSCs had a modest increase for both markers, ASCs expressed these factors in the appropriate sequentially-expressed manner; Myogenin peaked at almost 200-fold higher expression than undifferentiated cells followed by a near 25-fold peak in MEF2C after 3 and 5 days in culture, respectively, versus (Fig. 2, Middle). Osteogenic genes were also observed with early- and late-expressing factors TWIST and Osteocalcin, which correlated with cell mineralization. In accordance with early Runx2 expression (Fig. 1B), ASCs expressed peak levels of TWIST followed by Osteocalcin. BMSCs showed similar osteogenic trends but to significantly lower degree (Fig. 2, right). BMSCs did not show serum dependence with the exception of GDNF (Fig. 2, 10 vs. 20% serum). However, a comparison of ASCs on permissive and non-permissive matrices for each lineage indicated an average maximal difference of 40-fold, much greater than the less than 5-fold difference

for BMSCs (Fig. S3B). Thus ASCs appear to more robustly express specific lineage pathways when induced by matrix.

3.2. Matrix induced ASC fusion

The degree of myogenic gene expression observed here has not been previously observed with BMSCs [4, 25] or even those ASCs that undergo serum- and co-culture-dependent fusion [13, 27]. Fusion into a myotube is a terminal and well-documented step in myocyte maturation [28, 29] and given the strength of myogenic induction here, we asked if matrix stiffness could induce ASC fusion without specific growth factor- and co-culture-dependent cues. C2C12 myoblasts, ASCs, and BMSCs were singly labeled with either a green or red fluorescent membrane dye and subsequently mixed and cultured on myogenic matrices. Though all cell sources started with either green or red membranes (Fig. 3A, Left), after one week in culture, bi-nucleated ASCs were observed with green and red co-localized membranes (Fig. 3A, Middle). Similar membrane fusion was also found in C2C12 myoblasts after 4 days (Fig. 3A, Top), but although adjacent BMSCs were observed, no cell showed dye transfer, indicative of membrane fusion (Fig. 3A, Bottom). A hallmark of myocyte fusion is a continuous cytoskeleton [29], so β tubulin was used to assess cytoskeletal continuity in cells. After one week, 2.09 ± 0.35% of ASCs fused to bi-nucleated, elongated cells with a shared cytoskeleton (Fig. 3B, Top) reminiscent of myotubes. Lack of the cell proliferation marker, Ki67, indicated that these bi-nucleated cells were not the result of a proliferating cell after nuclear but before membrane fission, which could have accounted for bi-nucleation. ASC fusion could be disrupted by the myotube fission reagent, myoseverin [20], after 18 hours of exposure. As shown in the inset, fission also restores Ki67 expression in some cells as they return to their normal cell cycle (Fig. 3B, Middle). However myoseverin wash-out and another week of culture on myogenic matrices allowed ASCs to re-fuse at a rate of 1.62 ± 0.58%, which was statistically similar to their pre-treated value (Fig. 3B, Bottom).

Fibrotic muscle often is stiffer than normal such as in muscular dystrophy [1, 15]. To determine if one week old ASC-derived bi-nucleated cells could withstand a more rigid, fibrotic-like environment and demonstrate a lack of phenotype plasticity, cells were replated onto permissive firm matrix as well as non-permissive stiff matrix. After replating and an additional week on the 10 kPa matrix, 2.25 ± 0.40% of ASCs were multi-nucleated with a continuous cytoskeleton (Fig. 3C, Top), thus maintaining their previous state (Fig. 3B, Top). When replated onto the non-permissive 34 kPa matrix, a similar percentage of ASCs remained fused (Fig. 3C, Middle), showing that they could not reprogram themselves. However, those ASCs which were replated as single cells may retain some degree of plasticity as they showed punctate Runx2 staining (Fig. 3C, Bottom). Together these data suggest that when using multi-nucleated ASCs as a therapeutic cell source for fibrotic muscle, isolating them from singly-nucleated reprogrammable cells will be necessary.

3.3. Mechanosensitivity differences between ASCs and BMSCs

To confirm that fusion was induced by mechanical stimuli, cell contraction was activated or inhibited by the contractile agonist lysophosphatidic acid (LPA) [30] or the non-muscle myosin II (NMMII) inhibitor, blebbistatin (BLE), respectively [4, 31]. After 7 days, more LPA treated ASCs fused into multi-nucleated myotubes (3.63 ± 031% vs. 2.09 ± 0.35%) and BLE treatment reduced myotube fusion 4-fold (0.53 ± 0.13%) and even caused the few fused cells to lose their spindle morphology (Fig. 4A). Based on the commitment differences between ASCs and BMSCs, fusion regulation by NMMII, and NMMII's role in cell contraction and mechanosensing [32], we next determined how cells could differentially sense stiffness. ASCs expressed and assembled more b isoform of NMMII into striations compared to BMSCs (Fig. 4B) with striation distances being more regular in ASCs, which is

an indication of muscle maturation [33]. To determine if NMMIIb assembly affected force transduction in the cells, a 3-dimensional traction force microscopy (TFM) technique [22] was used to monitor how cells pulled on their surrounding matrix over time. Strain energy, which is an integration of the deformation over the entire cell (see representative images in Fig. 4C, Bottom), tended to be higher for ASCs than for BMSCs regardless of culture time (Fig. 4C, Top), which reflects the differences in differentiation trends (Fig. 2) and NMMIIb assembly (Fig. 4B).

Focal adhesions regulate a host of mechanically-sensitive processes as forces are transduced through them to the ECM [34], and one candidate sensor, vinculin, has been shown *in vitro* to unfold upon binding to stretched talin rod domains [35]. Thus we asked if vinculin was differentially assembled on the same time scale as differentiation differences were observed. After 3 days in culture on myogenic matrices, ASCs showed vinculin-containing adhesions at the cell periphery, which continued to mature over time (Fig. 5A, Top). On the other hand, BMSCs initially had poorly assembled vinculin-containing adhesions at the periphery, but after one week, adhesions resembled those in ASCs (Fig. 5A, Bottom). α5β1 and αVβ3 integrins are fibronectin receptors upstream of vinculin in focal adhesion signaling pathways [36]. Since ASCs here attach to fibronectin-bound matrices, we investigated their differentiation-dependence on α5 and αV integrin subunits. siRNA-mediated knockdown of each subunit for 4 days on tissue culture plastic did not prevent cell adhesion nor did it alter expression of the other integrin subunit (Fig. S4A); knockdown did reduce expression of the intended integrin subunit as much as 80–90% and was greater than 40% for up to 5 days in culture after plating onto myogenic matrices (Fig. 5B, Top and Fig. S4B). For both integrin α5 and αV knockdowns, ASCs failed to upregulate Myogenin and MEF2C compared to untreated cells (Fig. 5B, Bottom). However, ASCs allowed to recover for 4 days on tissue culture plastic instead of matrix regained their α5 or αV integrin expression (Fig. S4B) and, upon replating onto 10 kPa matrix, expressed nuclear-localized MyoD after 3 and 5 days of culture for α5 and αV integrin, respectively (Fig. S4C). Together these data indicate that specific differences in mechanosensor expression and force transduction may be responsible for differentiation differences in ASCs and BMSCs.

4. Discussion

BMSC differentiation has been well-documented by soluble as well as matrix-based methods [37]. Given the common mesenchymal signature of ASCs and BMSCs, we had thus expected stiffness to drive ASCs into precursor populations of various lineages based on matrix stiffness as with BMSCs [4, 25] and in contrast to lineage-specified cells, e.g. myocytes [15] and osteoblasts [38]. However, ASCs not only expressed important early transcriptional factors to a remarkably high level, they fused into multi-nucleated myotubes expressing mature muscle proteins. Furthermore, ASC-derived myotubes were able to remain fused when introduced to stiff niche that mimicked fibrotic muscle, a behavior never reported for BMSCs.

Our findings provide an improved method for generating myogenically-primed cells for transplantation which does not rely on methods requiring costly growth factors [27], co-cultured animal cells [13], or exceedingly high cell density [39]. Moreover, matrix stiffness appears to generate fused ASCs in a shorter period of time and at a rate nearly 10-fold higher than previously observed [13]. Recent genetic analyses have identified a common brown adipose/skeletal muscle precursor [40] where adipo- or myogenesis can be regulated with expression or repression of both PRDM16 [41] and MiR-193b-365 [42], respectively. When comparing myogenesis from our white fat-derived ASCs induced by ECM stiffness and PRDM16 inhibition of brown fat, stiffness still appears to produce higher gene expression in our ASCs. Perhaps the most important point in the context of our observations

is that these common approaches with ASCs and BMSCs do not appear to improve muscle function *in vivo* [10]. What may make ECM stiffness such a potent myogenic induction factor and ASC-derived myotubes ideal for translation in fibrotic muscle is that when stiffness induced-ASCs were replated onto non-permissive matrix, fused myotubes remained multi-nucleated rather than reprogramming themselves. Unlike BMSCs who retained some plasticity *in vitro* [4], fused ASCs did not appear to transdifferentiate though single ASCs did. Subsequent multi-factorial sorting based on size–multinucleated cells being larger–and expression of muscle-specific β1D and α7 integrins [43] could separate out ASC-derived myotubes from single cells for therapeutic treatment by muscle injection.

To understand the origin of why ASCs are different despite a similar initial state, one needs to look no further than the adhesive mechanisms used by these cell sources. Loss of either fibronectin-binding integrin pair would appear enough to halt ASC myogenesis, which has previously proven indispensible for BMSC fate [25]. Given that focal adhesion assembly appeared to be delayed in BMSCs, adhesions would appear all the more important to the early onset of lineage specification in ASCs. These integrins have contraction-dependent relaxed and tensioned states [44] that can induce focal adhesion signaling [35], so higher strain energy occurring earlier would imply greater activation of integrin-associated mechanosensitive pathways in ASCs, including differentiation. While the exact mechanism of sensing is still uncertain, most involve force transduction at adhesions [34, 36], providing a plausible explanation for ASCs “feeling” their niche more and faster than BMSCs.

Despite promising *in vitro* data, autologous stem cell injection in animal models has produced mixed results with the suggestion that fibrosis stiffens muscle [1] to decrease engraftment efficacy and alter cell fate [5, 6, 45]. Findings here suggest that abundant and easily isolated ASCs pre-committed by stiffness may be a more clinically viable source for stem cells in diseased skeletal muscle than other less abundant [11] or functionally-limited cell sources [9, 10]. These data strongly suggest that fully characterizing the ECM state of the diseased cell niche is essential prior to undertaking therapeutic intervention.

5. Conclusions

While mechanically-induced fate decisions of ASCs mirror BMSCs, their sensitivity and capacity to undergo myogenesis is dramatically improved through expressing sequential muscle transcriptional regulators and fusing into multi-nucleated tubes, which BMSCs do not. The mechanism underlying this difference involves their differential ability to assemble contractile proteins and transduce higher forces through better and faster-assembled focal adhesion. Most importantly for clinical applications, ASC-derived myotubes maintained their fused phenotype on non-permissive disease-like stiff matrix. These results imply enhanced mechanosensitivity for ASCs versus BMSCs, making them a better therapeutic cell source for skeletal muscle repair or tissue engineering.

Supplementary Material

Refer to Web version on PubMed Central for supplementary material.

Acknowledgments

The authors would like to thank Drs. Karen Christman and Shyni Varghese for surface receptor antibodies and reagents, respectively. This work was funded by the Human Frontier Science Program (RGY0064/2010) and NIH (1DP02 OD006460).

References

1. Stedman HH, Sweeney HL, Shrager JB, Maguire HC, Panettieri RA, Petrof B, et al. The mdx mouse diaphragm reproduces the degenerative changes of Duchenne muscular dystrophy. Nature. 1991; 352:536–539. [PubMed: 1865908]
2. Bushby K, Finkel R, Birnkrant DJ, Case LE, Clemens PR, Cripe L, et al. Diagnosis and management of Duchenne muscular dystrophy, part 1: diagnosis, and pharmacological and psychosocial management. Lancet Neurol. 2010; 9:77–93. [PubMed: 19945913]
3. Davies JE, Rose C, Sarkar S, Rubinsztein DC. Cystamine suppresses polyalanine toxicity in a mouse model of oculopharyngeal muscular dystrophy. Sci Transl Med. 2010; 2 34ra40.
4. Engler AJ, Sen S, Sweeney HL, Discher DE. Matrix elasticity directs stem cell lineage specification. Cell. 2006; 126:677–689. [PubMed: 16923388]
5. Breitbach M, Bostani T, Roell W, Xia Y, Dewald O, Nygren JM, et al. Potential risks of bone marrow cell transplantation into infarcted hearts. Blood. 2007; 110:1362–1369. [PubMed: 17483296]
6. Berry MF, Engler AJ, Woo YJ, Pirolli TJ, Bish LT, Jayasankar V, et al. Mesenchymal stem cell injection after myocardial infarction improves myocardial compliance. Am J Physiol Heart Circ Physiol. 2006; 290:H2196–H2203. [PubMed: 16473959]
7. Pittenger MF, Mackay AM, Beck SC, Jaiswal RK, Douglas R, Mosca JD, et al. Multilineage potential of adult human mesenchymal stem cells. Science. 1999; 284:143–147. [PubMed: 10102814]
8. Aggarwal S, Pittenger MF. Human mesenchymal stem cells modulate allogeneic immune cell responses. Blood. 2005; 105:1815–1822. [PubMed: 15494428]
9. Chan J, Waddington SN, O'Donoghue K, Kurata H, Guillot PV, Gotherstrom C, et al. Widespread distribution and muscle differentiation of human fetal mesenchymal stem cells after intrauterine transplantation in dystrophic mdx mouse. Stem Cells. 2007; 25:875–884. [PubMed: 17185606]
10. Gang EJ, Darabi R, Bosnakovski D, Xu Z, Kamm KE, Kyba M, et al. Engraftment of mesenchymal stem cells into dystrophin-deficient mice is not accompanied by functional recovery. Exp Cell Res. 2009; 315:2624–2636. [PubMed: 19460366]
11. Cerletti M, Jurga S, Witczak CA, Hirshman MF, Shadrach JL, Goodyear LJ, et al. Highly efficient, functional engraftment of skeletal muscle stem cells in dystrophic muscles. Cell. 2008; 134:37–47. [PubMed: 18614009]
12. Gilbert PM, Havenstrite KL, Magnusson KE, Sacco A, Leonardi NA, Kraft P, et al. Substrate elasticity regulates skeletal muscle stem cell self-renewal in culture. Science. 2010; 329:1078–1081. [PubMed: 20647425]
13. Di Rocco G, Iachininoto MG, Tritarelli A, Straino S, Zacheo A, Germani A, et al. Myogenic potential of adipose-tissue-derived cells. J Cell Sci. 2006; 119:2945–2952. [PubMed: 16825428]
14. Liu Y, Yan X, Sun Z, Chen B, Han Q, Li J, et al. Flk-1+ adipose-derived mesenchymal stem cells differentiate into skeletal muscle satellite cells and ameliorate muscular dystrophy in mdx mice. Stem Cells Dev. 2007; 16:695–706. [PubMed: 17999592]
15. Engler AJ, Griffin MA, Sen S, Bonnemann CG, Sweeney HL, Discher DE. Myotubes differentiate optimally on substrates with tissue-like stiffness: pathological implications for soft or stiff microenvironments. J Cell Biol. 2004; 166:877–887. [PubMed: 15364962]
16. McBeath R, Pirone DM, Nelson CM, Bhadriraju K, Chen CS. Cell shape, cytoskeletal tension, and RhoA regulate stem cell lineage commitment. Developmental Cell. 2004; 6:483–495. [PubMed: 15068789]
17. Zuk PA, Zhu M, Mizuno H, Huang J, Futrell JW, Katz AJ, et al. Multilineage cells from human adipose tissue: implications for cell-based therapies. Tissue Eng. 2001; 7:211–228. [PubMed: 11304456]
18. Choi YS, Dusting GJ, Stubbs S, Arunothayaraj S, Han XL, Collas P, et al. Differentiation of human adipose-derived stem cells into beating cardiomyocytes. J Cell Mol Med. 2010; 14:878–889. [PubMed: 20070436]
19. Choi YS, Matsuda K, Dusting GJ, Morrison WA, Dilley RJ. Engineering cardiac tissue in vivo from human adipose-derived stem cells. Biomaterials. 2010; 31:2236–2242. [PubMed: 20031204]

20. Rosania GR, Chang YT, Perez O, Sutherlin D, Dong H, Lockhart DJ, et al. Myoseverin, a microtubule-binding molecule with novel cellular effects. Nat Biotechnol. 2000; 18:304–308. [PubMed: 10700146]
21. Tse JR, Engler AJ. Preparation of hydrogel substrates with tunable mechanical properties. Curr Protoc Cell Biol. 2010; Chapter 10(Unit 10):6.
22. Del Alamo JC, Meili R, Alonso-Latorre B, Rodriguez-Rodriguez J, Aliseda A, Firtel RA, et al. Spatio-temporal analysis of eukaryotic cell motility by improved force cytometry. Proc Natl Acad Sci U S A. 2007; 104:13343–13348. [PubMed: 17684097]
23. Flanagan LA, Ju YE, Marg B, Osterfield M, Janmey PA. Neurite branching on deformable substrates. Neuroreport. 2002; 13:2411–2415. [PubMed: 12499839]
24. Galante LL, Schwarzbauer JE. Requirements for sulfate transport and the diastrophic dysplasia sulfate transporter in fibronectin matrix assembly. J Cell Biol. 2007; 179:999–1009. [PubMed: 18056413]
25. Rowlands AS, George PA, Cooper-White JJ. Directing osteogenic and myogenic differentiation of MSCs: interplay of stiffness and adhesive ligand presentation. Am J Physiol Cell Physiol. 2008; 295:C1037–C1044. [PubMed: 18753317]
26. Guilak F, Cohen DM, Estes BT, Gimble JM, Liedtke W, Chen CS. Control of stem cell fate by physical interactions with the extracellular matrix. Cell Stem Cell. 2009; 5:17–26. [PubMed: 19570510]
27. Zuk PA, Zhu M, Ashjian P, De Ugarte DA, Huang JI, Mizuno H, et al. Human adipose tissue is a source of multipotent stem cells. Mol Biol Cell. 2002; 13:4279–4295. [PubMed: 12475952]
28. Yaffe D, Saxel O. Serial passaging and differentiation of myogenic cells isolated from dystrophic mouse muscle. Nature. 1977; 270:725–727. [PubMed: 563524]
29. Taylor MV. Muscle differentiation: how two cells become one. Curr Biol. 2002; 12:R224–R228. [PubMed: 11909553]
30. Ohata H, Niioka T, Kim MS, Ando S, Yamamoto M, Momose K. Role of lysophosphatidic acid as a mechanosensitizer. Nihon Yakurigaku Zasshi. 2004; 124:329–335. [PubMed: 15502398]
31. Straight AF, Cheung A, Limouze J, Chen I, Westwood NJ, Sellers JR, et al. Dissecting temporal and spatial control of cytokinesis with a myosin II Inhibitor. Science. 2003; 299:1743–1747. [PubMed: 12637748]
32. Rosenfeld SS, Xing J, Chen LQ, Sweeney HL. Myosin IIb is unconventionally conventional. J Biol Chem. 2003; 278:27449–27455. [PubMed: 12740390]
33. Sanger JW, Chowrashi P, Shaner NC, Spalthoff S, Wang J, Freeman NL, et al. Myofibrillogenesis in skeletal muscle cells. Clin Orthop Relat Res. 2002:S153–S162. [PubMed: 12394464]
34. Geiger B, Spatz JP, Bershadsky AD. Environmental sensing through focal adhesions. Nat Rev Mol Cell Biol. 2009; 10:21–33. [PubMed: 19197329]
35. del Rio A, Perez-Jimenez R, Liu R, Roca-Cusachs P, Fernandez JM, Sheetz MP. Stretching single talin rod molecules activates vinculin binding. Science. 2009; 323:638–641. [PubMed: 19179532]
36. Vogel V, Sheetz M. Local force and geometry sensing regulate cell functions. Nat Rev Mol Cell Biol. 2006; 7:265–275. [PubMed: 16607289]
37. Discher DE, Mooney DJ, Zandstra PW. Growth factors, matrices, and forces combine and control stem cells. Science. 2009; 324:1673–1677. [PubMed: 19556500]
38. Hicok KC, Du Laney TV, Zhou YS, Halvorsen YD, Hitt DC, Cooper LF, et al. Human adipose-derived adult stem cells produce osteoid in vivo. Tissue Eng. 2004; 10:371–380. [PubMed: 15165454]
39. Vieira NM, Brandalise V, Zucconi E, Jazedje T, Secco M, Nunes VA, et al. Human multipotent adipose-derived stem cells restore dystrophin expression of Duchenne skeletal-muscle cells in vitro. Biol Cell. 2008; 100:231–241. [PubMed: 17997718]
40. Schulz TJ, Huang TL, Tran TT, Zhang H, Townsend KL, Shadrach JL, et al. Identification of inducible brown adipocyte progenitors residing in skeletal muscle and white fat. Proc Natl Acad Sci U S A. 2011; 108:143–148. [PubMed: 21173238]
41. Seale P, Bjork B, Yang W, Kajimura S, Chin S, Kuang S, et al. PRDM16 controls a brown fat/skeletal muscle switch. Nature. 2008; 454:961–967. [PubMed: 18719582]

42. Sun L, Xie H, Mori MA, Alexander R, Yuan B, Hattangadi SM, et al. Mir193b-365 is essential for brown fat differentiation. Nat Cell Biol. 2011; 13:958–965. [PubMed: 21743466]

43. Belkin AM, Retta SF, Pletjushkina OY, Balzac F, Silengo L, Fassler R, et al. Muscle beta1D integrin reinforces the cytoskeleton-matrix link: modulation of integrin adhesive function by alternative splicing. J Cell Biol. 1997; 139:1583–1595. [PubMed: 9396762]

44. Friedland JC, Lee MH, Boettiger D. Mechanically activated integrin switch controls alpha5beta1 function. Science. 2009; 323:642–644. [PubMed: 19179533]

45. Murry CE, Soonpaa MH, Reinecke H, Nakajima H, Nakajima HO, Rubart M, et al. Haematopoietic stem cells do not transdifferentiate into cardiac myocytes in myocardial infarcts. Nature. 2004; 428:664–668. [PubMed: 15034593]

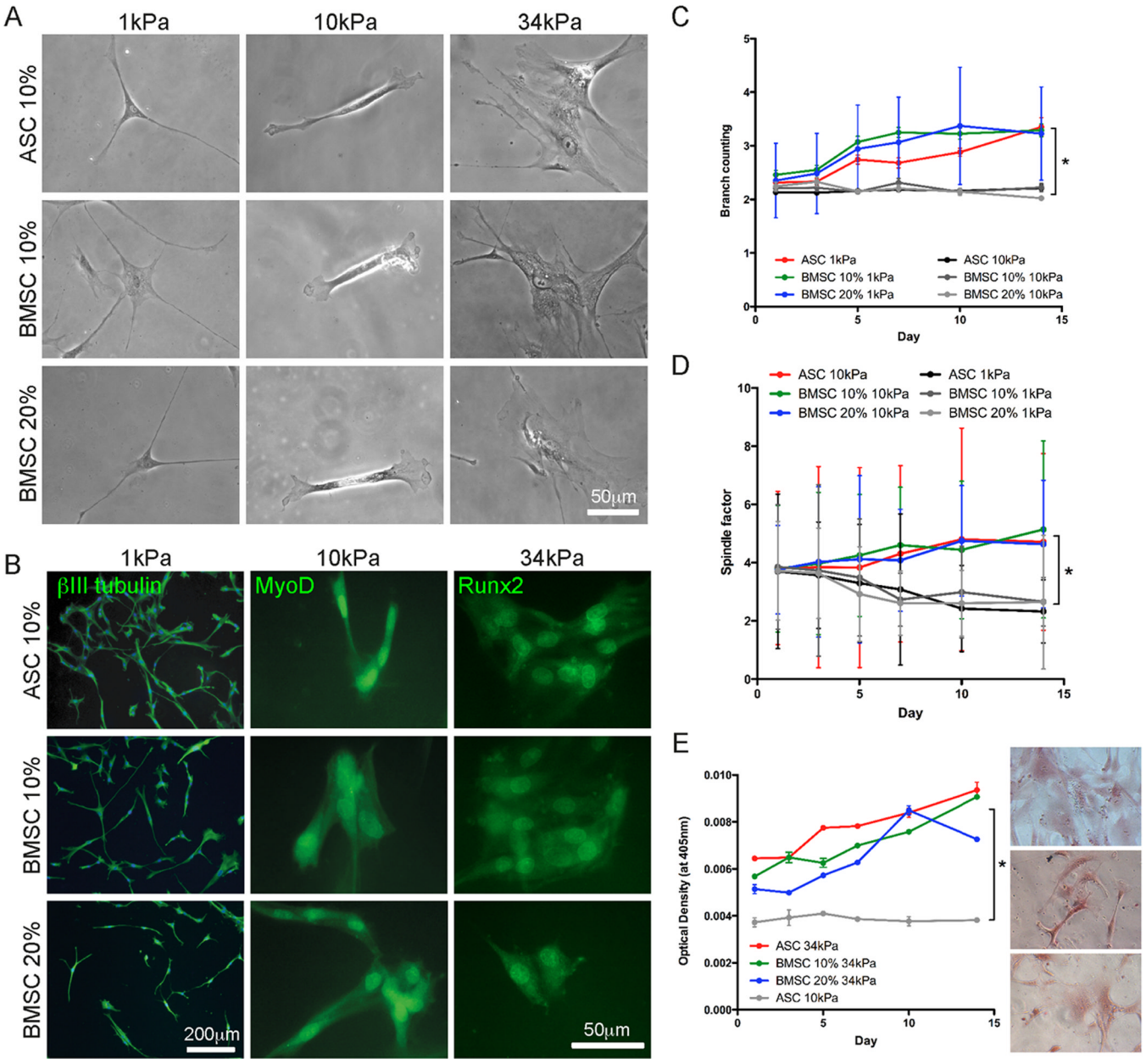

Fig. 1.

ASC and BMSC differentiation on matrices with lineage-specific stiffness. (A) Representative morphology in phase contrast and (B) lineage-specific marker expression in fluorescence (βIII tubulin for neurogenic, MyoD for myogenic, and Runx2 for osteogenic lineages) in ASCs and BMSCs cultured in the indicated matrix and serum conditions after 1 week in culture. (C) The number of branches that ASCs and BMSCs formed over 2 weeks in culture in the indicated matrix and serum conditions was quantified. (D) The spindle-shaped morphology of muscle was determined by a spindle factor, the major axis/minor axis of cell, for ASCs and BMSCs over 2 weeks in culture in the indicated matrix and serum conditions. (E) ASCs and BMSCs were stained for Alizarin Red S mineralization over 2 weeks in culture in the indicated matrix and serum conditions. Inset images are representative of ASCs (top) and BMSCs (10 and 20% serum, middle and bottom, respectively) cultured on

the 34 kPa matrix. All data shown in mean ± standard deviation for triplicate experiments. *$P < 0.05$.

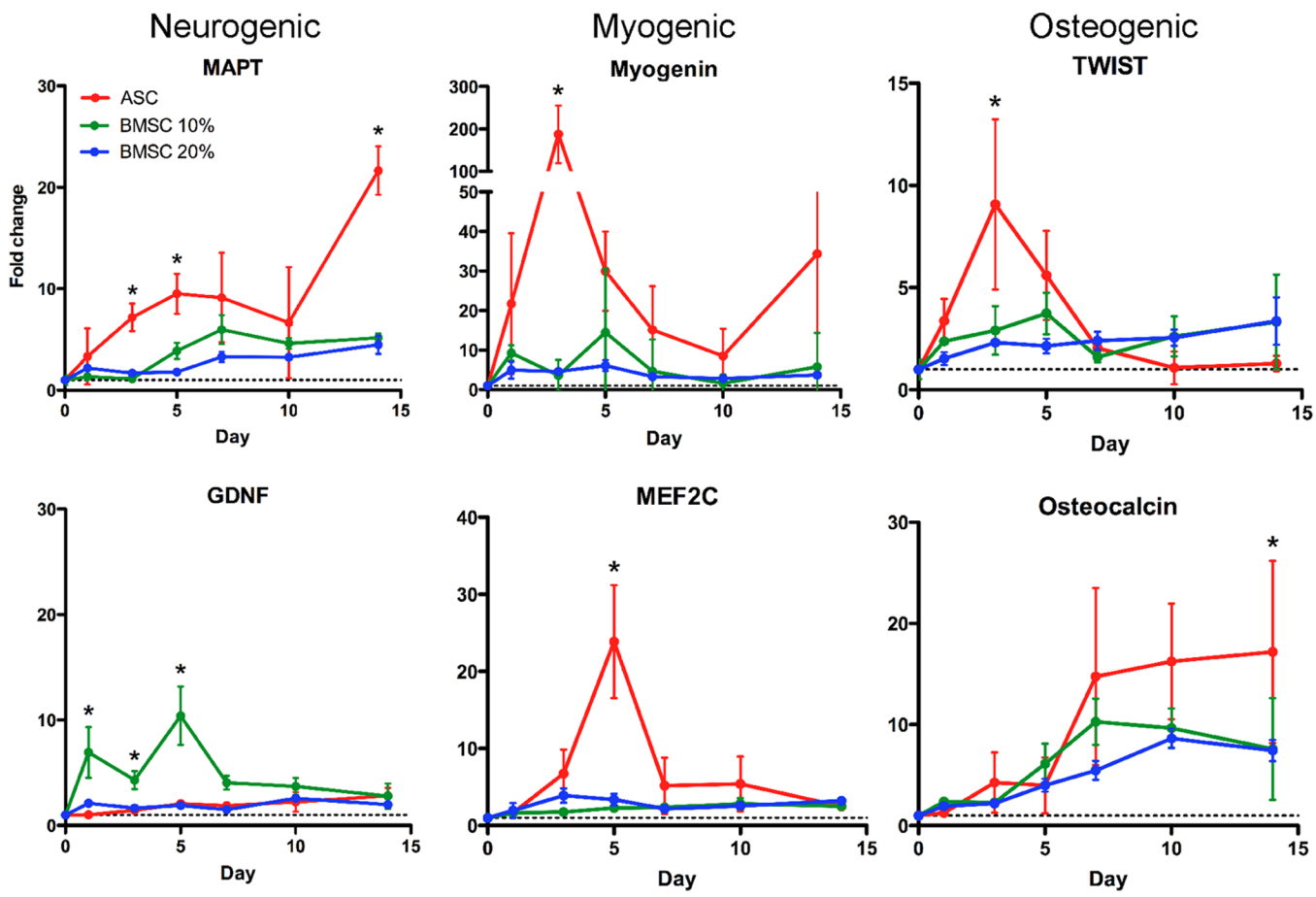

Fig. 2.

Lineage-specific mRNA is highest in ASCs. Gene expression of MAPT, GDNF, Myogenin, MEF2C, TWIST, and Osteocalcin was assessed by qPCR. Lineages are indicated at the top of each column. Expression was monitored as a function of time for ASCs cultured in 10% serum-containing media (red) and BMSCs cultured in either 10 (green) or 20% serum-containing media (blue). The dashed line indicates expression in the undifferentiated cell to which all data is normalized. * indicated $P < 0.05$.

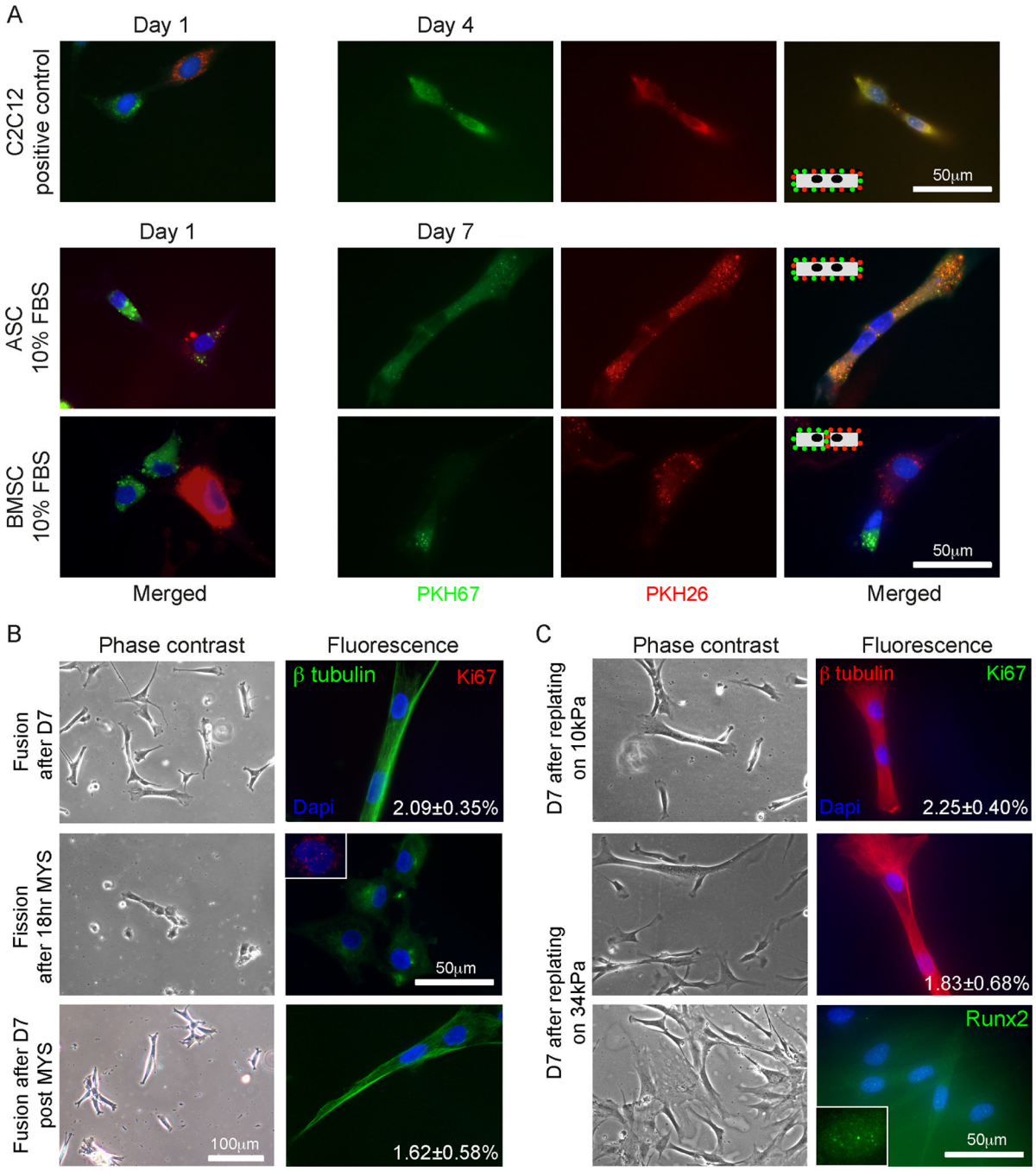

Fig. 3.

Multi-nucleated cell formation in ASCs on myogenic matrices. (A) PKH67 (green) and PKH26 (red) labeled C2C12 myoblasts (top), ASCs (middle), and BMSCs (bottom) were mixed with their oppositely labeled cell of the same type, plated on 10kPa matrix, and monitored for dye transfer between cells. After 1 day, all three cell sources did not exhibit transfer between adjacent cells (left). Transfer between adjacent myotubes occurred by day4, between adjacent ASCs by day 7, and never occurred for BMSCs (right). The inset schematics illustrate this process. (B) ASCs were also examined by β tubulin (green, continuous cytoskeleton) and Ki67 (red, proliferation) after day 7. The percent of bi-nucleated cells is inset in the fluorescent image (top). Myoseverin was added to cells after

day 7, reverting bi-nucleated cells to singly-nucleated cells (middle), with some Ki67 positive staining (inset). After washout, ASCs refused at a rate similar to the pre-treated cells as indicated (bottom). (C) After 7 days in culture on 10kPa matrix, ASCs were replated onto either 10 (top) or 34 kPa matrices (middle and bottom) for an additional 7 days. The percent of bi-nucleated cells is inset in the fluorescent images stained for β tubulin (red) and ki67(green). Singly-nucleated cells replated from 10 to 34 kPa were also stained for Runx2 (green, bottom and inset).

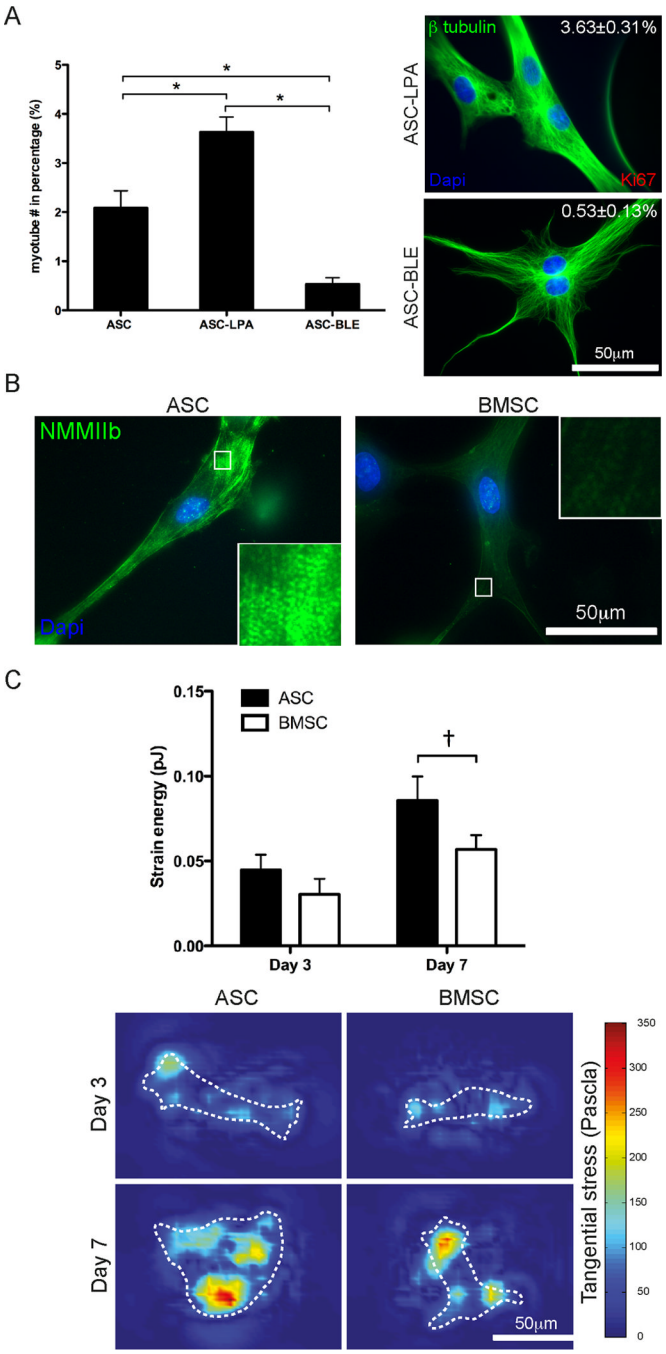

Fig. 4.

Mechanotransduction in ASCs and BMSCs regulates differentiation. (A) Myotube frequency was increased by the contractile agonist Lysophosphatidic acid (LPA) and decreased by the NMMII inhibitor Blebbistatin (BLE). *P < 0.001. (B) Immunofluorescent staining of NMMIIb in ASCs and BMSCs with higher magnification images inset to illustrate striation assembly. (C) Strain energy was measured by TFM (top). Representative images of the tangential stress (bottom) generated from TFM are shown at both days 3 and 7 with white cell outlines. The colormap indicates the magnitude of the stress as measured in Pascals. Data is reported as the mean ± standard error from triplicate experiments representing greater than 12 cells. †P = 0.07.

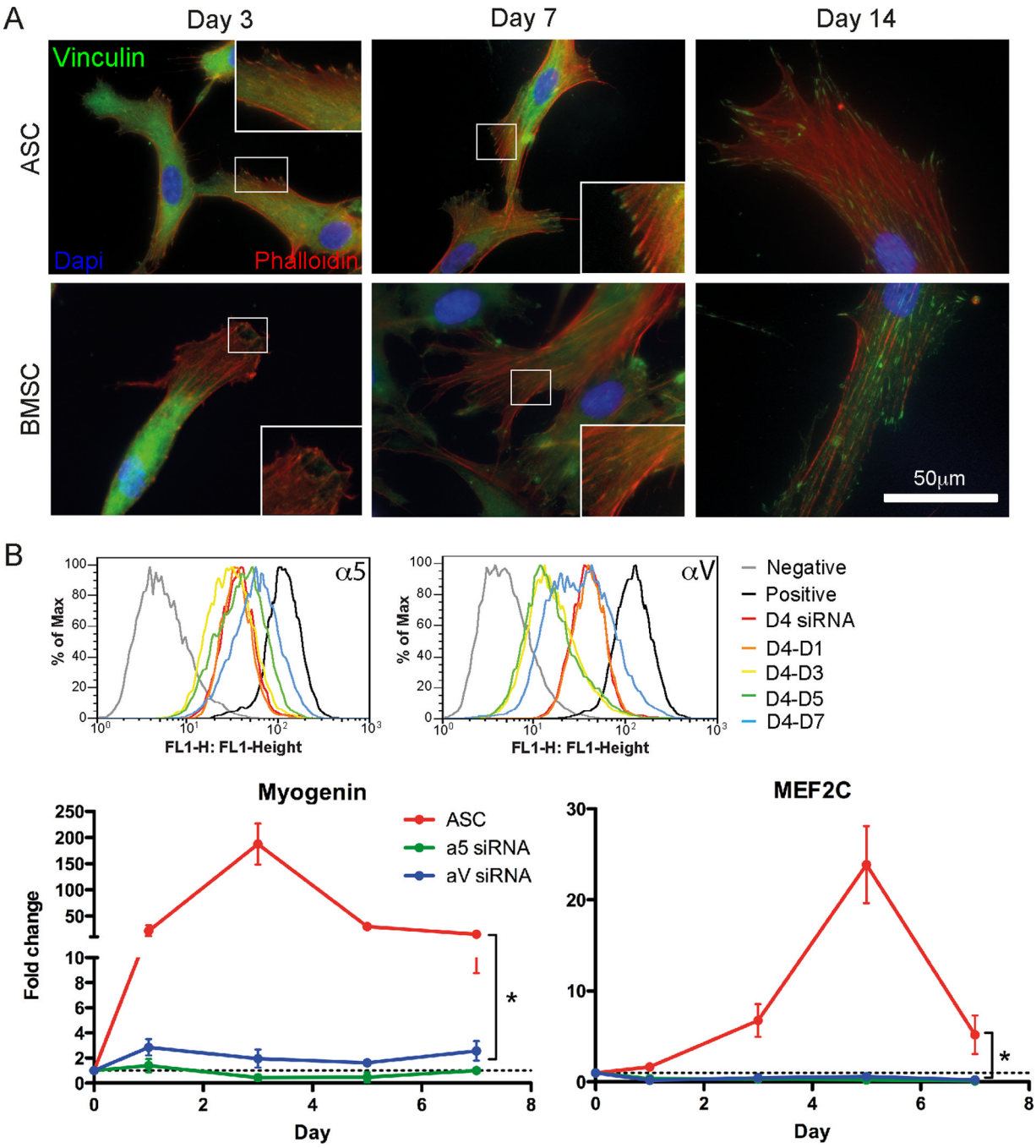

Fig. 5.

Mechanical induction is differentially transduced by intracellular signals via focal adhesions. (A) Assembled vinculin adhesions (green) were found in ASCs (left) at day 3 and in BMSCs (right) by day 7. F-actin (red phalloidin) and nuclei (blue) are also shown. (B) Flow cytometry plots of ASCs transfected with siRNA for α5 (top)or αV integrin (bottom) on TCP for 4 days (D4 siRNA) or ASCs that were also then replated on myogenic 10kPa matrices for the indicate time in days (left). qPCR analysis of myogenic markers Myogenin and MEF2C showed total inhibition for siRNA-treated cells of either integrin. Data represents the mean ± standard deviation of triplicate experiments. *P < 0.05.